Hierarchical Control of End-Point Impedance and Joint Impedance for Redundant Manipulators

Toshio Tsuji, Achmad Jazidie, and Makoto Kaneko, *Member, IEEE*

***Abstract*—This paper proposes an impedance control method for redundant manipulators, which can control not only the end-point impedance using one of the conventional impedance control methods, but the joint impedance which has no effects on the end-point impedance. First, a sufficient condition for the joint impedance controller is derived. Then, the optimal controller for a given desired joint impedance is designed using the least squares method. Finally, computer simulations and experiments using a planar direct-drive robot are performed in order to confirm the validity of the proposed method.**

***Index Terms*—Impedance control, manipulators, redundancy, robot dynamics.**

I. Introduction

IMPEDANCE control [1] provides a unified approach for position and force control of a manipulator, where a controlled variable is a dynamic relation between motion and force. Using the motion equation of the manipulator and measurements of the manipulator's motion, this method can regulate the end-point impedance to the desired value which is designed depending on a given task. To date, many studies on impedance control have been conducted. Hogan [2] has proposed a method to implement impedance control without the calculation of an inverse of the Jacobian matrix. Tachi *et al*. [3] have developed an impedance control method that does not require the use of a force sensor. The robustness of impedance control for uncertainties such as modeling errors and disturbances has been discussed in [4], [5], and the stability of a manipulator performing a contact task has been analyzed in [6], [7].

In addition, a redundant manipulator which possesses more degrees of freedom than the ones required for performing a task has been considered to be the key to more dextrous and versatile robot motions. Many studies on arm redundancy have been performed in terms of the inverse kinematic problem [8]–[13], where arm redundancy is used in order to optimize criteria such as avoidance of singularity [10], avoidance of an obstacle [11]–[13], and various measures of dexterity [10], [12]. Also, redundancy in the force/torque transformation has been pointed out by Khatib [14], [15] and Kang and Freeman [16].

Manuscript received October 1, 1997; revised January 24, 1999 and June 2, 1999.

T. Tsuji and M. Kaneko are with the Department of Industrial and Systems Engineering, Hiroshima University, Higashi-Hiroshima, 739-8527 Japan.

A. Jazidie is with the Electrical Engineering Department, Surabaya Institute of Technology, Surabaya, 60111 Indonesia.

Publisher Item Identifier S 1083-4427(99)06985-4.

With regard to impedance control, a number of studies on the utilization of kinematic redundancy has been reported thus far [17]–[24]. Newman and Dohring [17] proposed the augmented impedance control method based on the extended Jacobian scheme developed by Baillieul [13]. In this scheme, a vector of new task variables with its dimension equal to the degrees of freedom of the kinematic redundancy is defined and augmented to the end-point position vector to make the Jacobian matrix square. By using the augmented Jacobian matrix, the impedance control law which satisfies a constraint expressed by the extended Jacobian matrix is derived. However, this method does not take inertial effects into account, so it reduces to the active stiffness control [25] rather than the impedance control. Later, Peng and Adachi [18] introduced a differentiable scalar objective function of joint angles, and derived the end-point impedance control law that optimizes the objective function. Using this control method, the kinematic redundancy can be utilized to control the arm configuration while controlling the end-point impedance. Also, Oh *et al*. [19] described the dynamics of the redundant manipulator in a task space including null space motion, and defined the desired inertia and viscosity for the null space dynamics as well as the hybrid impedance [26] for position and force controlled directions. The physical meaning of the impedance for the null space dynamics expressed in the task space, however, is not intuitively understood. Therefore, the planning of the desired null space impedance according to a given task may be a difficult problem. Also the stiffness is not included in the null space impedance parameters.

Our approach is significantly different from others. We have argued that the arm redundancy should be directly utilized in terms of the arm impedance itself [20], and proposed an impedance control method named *Multi-Point Impedance Control* (MPIC) [21]–[23]. The MPIC can control not only the end-point impedance using one of the conventional impedance control methods but also impedances of multiple points on the links of the manipulator utilizing arm redundancy. On the basis of the same idea, Liao and Donath [24] proposed the generalized impedance control for collision avoidance. Instead of the multi-point impedance, this paper proposes a method for controlling the joint impedance directly which has no effects on the end-point impedance.

Let us consider, as an example, a redundant manipulator performing a task that requires a compliant end-point motion as shown in Fig. 1(a), where the end-effector and a part of the arm are below the surface of the water. Various hydrodynamic forces caused by fluid such as the effects of added mass,

1083–4427/99$10.00 © 1999 IEEE

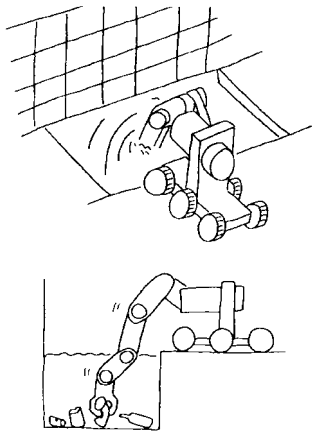

(a)

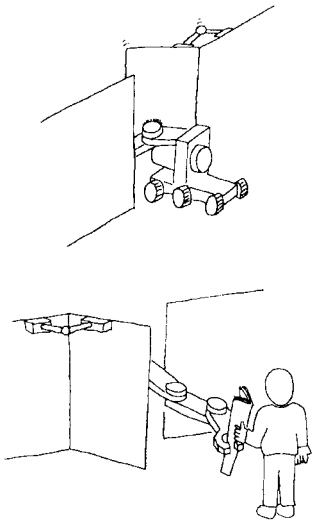

(b)

Fig. 1. Examples of tasks requiring impedance control of joints as well as the end-point.

drag and lift forces and buoyancy forces are exerted on the manipulator in underwater environments [27]. Although the previously proposed end-point impedance control methods can regulate the dynamic responses of the end-point motion for unknown external disturbances applied to the end-point, they are incompetent for disturbances applied to the links or the joints of the manipulators. In the presence of such disturbances, the joint configuration of the manipulator may change even if the end-point impedance is properly controlled, and it may result in serious accidents such as a collision with an obstacle or a singular joint configuration.

One possible solution to this problem is to set the impedance of specific joints under the water to be as large as possible in order to lock out the corresponding joints while controlling the end-point impedance to the given desired value. It could be possible to lock the underwater joints mechanically and use the conventional nonredundant impedance control for the rest of the joints. However, since both the kinematics and the dynamics of the manipulator are affected by locking the joints, the impedance control law should be modified depending on the number of locked joints and the arm posture which are not always constant during the task. We need to develop a unified scheme that can control the joint impedance as well as the end-point impedance utilizing kinematic redundancy. Also the same problem may arise for a manipulator bracing against an object, e.g., a door, at a joint or a link as shown in Fig. 1(b). In this case, the impedance of the joints located between the base of the manipulator and the contact point with the object should be regulated to be as stiff as possible.

In this paper, a new impedance control method for redundant manipulators is developed, which can realize the closest joint impedance to the desired one in the least squares sense while still satisfying the desired end-point impedance. Under this impedance control, the desired joint impedance and the desired joint angle, that is, the equilibrium arm posture, can be specified, and the end-point impedance and the joint impedance are hierarchically controlled. Control of the joint impedance enables us to regulate the dynamic response of the joints for the unknown external forces beforehand.

This paper is organized as follows: in Section II, a joint impedance controller is incorporated into the end-point impedance controller in parallel, and a sufficient condition of the joint impedance controller so as not to affect the end-point impedance is derived. In Section III, the joint impedance controller corresponding to the desired joint impedance is derived using the least squares method. Computer simulations and experiments using a planar direct-drive robot are performed in Section IV in order to show the effectiveness of the proposed method.

II. Impedance Control Utilizing Kinematic Redundancy

In general, the motion equation of an m-joint manipulator can be expressed as

$$M(\theta)\ddot{\theta} + h(\theta, \dot{\theta}) = \tau + J^T(\theta) F_{\text{ext}} \tag{1}$$

where

$F_{\text{ext}} \in \Re^l$	external force exerted on the end-point;
$\theta \in \Re^m$	joint angle vector;
$M(\theta) \in \Re^{m \times m}$	nonsingular inertia matrix (hereafter denoted by M);
$h(\theta, \dot{\theta}) \in \Re^m$	nonlinear term including the joint torque due to the centrifugal, Coriolis, gravitational, and frictional forces;
$\tau \in \Re^m$	joint torque vector;
$J(\theta) \in \Re^{l \times m}$	Jacobian matrix (hereafter denoted by J);
l	dimension of the task space.

For a redundant manipulator, m is larger than l.

The desired impedance of the end-point is generally expressed as

$$M_e \ddot{X} + B_e \, d\dot{X} + K_e \, dX = F_{\text{ext}} \tag{2}$$

where M_e, B_e, $K_e \in \Re^{l \times l}$ are the desired inertia, viscosity, and stiffness matrices of the end-point, respectively; and $dX = X - X_d \in \Re^l$ is the deviation vector of the end-point position X from its equilibrium X_d.

In this paper, we adopt the impedance control law not using the inverse of the Jacobian matrix [2]:

$$\tau = \tau_{\text{effector}} + \tau_{\text{comp}} \tag{3}$$

$$\tau_{\text{effector}} = -J^T[\Lambda\{M_e^{-1}(K_e\, dX + B_e\, d\dot{X}) + \dot{J}\dot{\theta}\} + \{I - \Lambda M_e^{-1}\}F_{\text{ext}}] \tag{4}$$

$$\tau_{\text{comp}} = (J^+_{M^{-1}}J)^T\hat{h}(\theta,\dot{\theta}) \tag{5}$$

where $\Lambda = (J\hat{M}^{-1}J^T)^{-1} \in \Re^{l\times l}$ is the operational space kinetic energy matrix [14], [15]; $J^+_{M^{-1}} = \hat{M}^{-1}J^T\Lambda \in \Re^{m\times l}$ the generalized inverse of J weighted by $\hat{M}^{-1}$; $\tau_{\text{effector}} \in \Re^m$ the joint torque vector needed to produce the desired end-point impedance; I the $l \times l$ unit matrix; and $\tau_{\text{comp}} \in \Re^m$ the joint torque vector for nonlinear compensation. Also, $\hat{M}(\theta)$ and $\hat{h}(\theta,\dot{\theta})$ are the estimated values of $M(\theta)$ and $h(\theta,\dot{\theta})$. It is assumed in this paper that the joint configuration θ is not in a singular posture, and $\hat{M}(\theta) = M(\theta)$ and $\hat{h}(\theta,\dot{\theta}) = h(\theta,\dot{\theta})$ are held.

Although the control law (3)–(5) and other impedance control methods such as [1], [3] can be applied to redundant manipulators, arm redundancy cannot be effectively utilized. In this paper, an additional controller is incorporated into the end-point impedance control law in order to exploit the arm redundancy

$$\tau = \tau_{\text{add}} + \tau_{\text{effector}} + \tau_{\text{comp}} \tag{6}$$

where $\tau_{\text{add}} \in \Re^m$ is the joint control torque vector for an additional purpose. It can be easily shown that if the additional joint control torque τ_{add} satisfies the equation

$$(J^+_{M^{-1}})^T\tau_{\text{add}} = 0 \tag{7}$$

then τ_{add} has no dynamical effects on the end-point motion of the manipulator, so that the end-point impedance remains equal to the desired one given by (2). This force redundancy was found by Khatib [14], [15], after which Kang and Freeman [16] used the force redundancy to assure stability in a joint torque optimization for the redundant manipulator by introducing the null-space damping technique. In the following sections, we present a method to utilize the force redundancy in terms of the joint impedance control.

III. Joint Impedance Regulation

A. Optimal Additional Controller

Equation (7) gives the sufficient condition for the additional joint torque τ_{add} to have no effect on the end-point's motion. In this subsection, we assume that the desired value of the additional torque τ^*_{add} is given, which does not always satisfy (7). We then need to derive τ_{add} that satisfies (7) and is the closest to the desired joint torque τ^*_{add}.

The general solution of (7) is given by

$$\tau_{\text{add}} = \{I_m - \Omega(J^+_{M^{-1}})^T\}z_1 \tag{8}$$

where I_m is the $m \times m$ unit matrix; $z_1 \in \Re^m$ an arbitrary constant vector; and $\Omega = J^+_{M^{-1}}\{(J^+_{M^{-1}})^TJ^+_{M^{-1}}\}^{-1} \in \Re^{m\times l}$ the right-side generalized inverse of $(J^+_{M^{-1}})^T$. The additional joint torque τ_{add} in (8) always satisfies the sufficient condition (7). The vector z_1 is then chosen in such a way that the following cost function $G_1(z_1)$ is minimized:

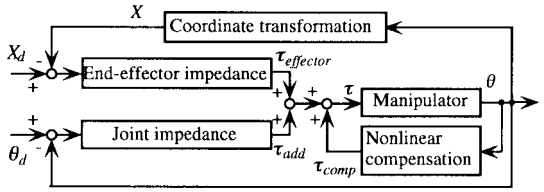

Fig. 2. Hierarchical impedance control for redundant manipulators.

$$G_1(z_1) = \|W\{\tau^*_{\text{add}} - \tau_{\text{add}}(Z_1)\}\| \tag{9}$$

where $W \in \Re^{m\times m}$ is a diagonal positive definite matrix, each diagonal element of which is a weight to the corresponding element of the joint torque error vector $\tau^*_{\text{add}} - \tau_{\text{add}}$, and $\|a\|$ stands for the Euclidian norm of the vector a

$$\|a\| = (a^Ta)^{1/2} = \left(\sum_{i=1}^{m} a_i^2\right)^{1/2} \tag{10}$$

where a_i is the ith element of vector $a \in \Re^m$. Using the least squares method, we can find the optimal solution given as

$$\tau_{\text{add}} = \Gamma\tau^*_{\text{add}} \tag{11}$$

$$\Gamma = I_m - \{\Omega_{W^{-2}}(J^+_{M^{-1}})^T\} \tag{12}$$

where $\Omega_{W^{-2}} = W^{-2}J^+_{M^{-1}}\{J^+_{M^{-1}}W^{-2}(J^+_{M^{-1}})^T\}^{-1} \in \Re^{m\times l}$ is the right-side generalized inverse of $(J^+_{M^{-1}})^T$ weighted by $W^{-2} \equiv W^{-1}W^{-1}$. As a result, using (4)–(6), (11), and (12), we can control not only the end-point impedance but the joint torque which is the closest to the given desired one without any effects on the end-point's motion.

B. Joint Impedance Control

It is then assumed that the desired joint impedance is given according to the task. The desired joint torque for the joint impedance regulation can be defined as

$$\tau^*_{\text{add}} = -M^*_j\ddot{\theta} - B^*_j\, d\dot{\theta} - K^*_j\, d\theta \tag{13}$$

where M^*_j, B^*_j, $K^*_j \in \Re^{m\times m}$ are the desired joint inertia, viscosity, and stiffness matrices, respectively, and $d\theta = \theta - \theta_d \in \Re^m$ is the deviation vector between the joint angle θ and its equilibrium one θ_d. Using (11)–(13), we can control the joint impedance as a subtask which has no effects on the end-point's motion (see Fig. 2).

The joint impedance realized by this control scheme, however, may differ from the desired one, since the proposed impedance control does not always achieve the desired joint torque. The property of the realized joint impedance is analyzed in the rest of this section.

First, the realized joint impedance related with the additional joint torque is expressed as

$$\tau_{\text{add}} = -M_j\ddot{\theta} - B_j\, d\dot{\theta} - K_j\, d\theta \tag{14}$$

where M_j, B_j, $K_j \in \Re^{m\times m}$ are the realized joint inertia, viscosity and stiffness matrices, respectively. It is easily seen

that the sufficient condition (7) is always satisfied if the following conditions are given:

$$(J^+_{M-1})^T M_j = 0, \tag{15}$$

$$(J^+_{M-1})^T B_j = 0 \tag{16}$$

$$(J^+_{M-1})^T K_j = 0. \tag{17}$$

For the joint inertia matrix M_j, the general solution of the matrix (15) is given as

$$M_j = \{I_m - \Omega (J^+_{M-1})^T\} Z_2 \tag{18}$$

where $Z_2 \in \Re^{m\times m}$ is an arbitrary constant matrix. The desired joint inertia matrix M_j^* is already given, so the problem is how to find an arbitrary constant matrix Z_2 in (18) which results in M_j close to M_j^*. To solve this problem, the following cost function $G_2(Z_2)$ is minimized with respect to Z_2:

$$G_2(Z_2) = \|W\{M_j^* - M_j(Z_2)\}\| \tag{19}$$

where $W \in \Re^{m\times m}$ is a diagonal positive definite matrix, each diagonal element of which acts as a weight for the corresponding row of the error matrix between M_j^* and M_j. The $\|A\|$ stands for the matrix norm defined by

$$\|A\| = (\mathrm{tr}[A^T A])^{1/2} = \left(\sum_{i=1}^{m} \sum_{j=1}^{m} a_{ij}^2 \right)^{1/2} \tag{20}$$

where $A = [a_{ij}] \in \Re^{m\times m}$ is an arbitrary matrix; and tr[·] denotes the trace of the matrix. Using the least squares method, we can find the optimal solution given as (see Appendix A)

$$M_j = \Gamma M_j^* \tag{21}$$

where Γ is given in (12). In the same manner, we can also derive the optimal solutions for the joint viscosity matrix B_j and the joint stiffness matrix K_j:

$$B_j = \Gamma B_j^*, \tag{22}$$

$$K_j = \Gamma K_j^*. \tag{23}$$

Obviously, the additional joint control torque (14) with M_j, B_j, K_j defined by (21)–(23) is exactly the same as the control law (11)–(13). This means that the proposed method always realizes the optimal joint impedance in a sense that the realized joint impedance is the closest to the desired joint impedance while achieving the desired end-point impedance.

C. Positive Semidefinite Joint Impedance

For a redundant manipulator, even if the stability of the end-point impedance is guaranteed, it does not mean that the joint motion is always stable. In this subsection, the joint impedance controller that assures the stability of the joint motion is derived on the basis of the positive semidefinitness of the joint impedance matrices M_j, B_j, and K_j.

In general, the positive semidefinitness of $M_j \in \Re^{m\times m}$ can be assured if it is expressed in the form

$$M_j = D_j D_j^T \tag{24}$$

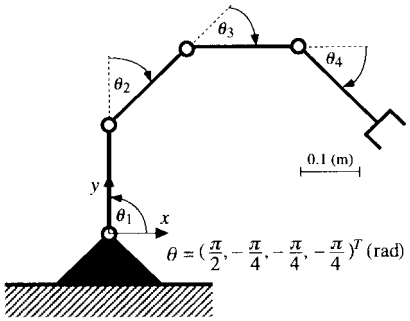

Fig. 3. Four-joint planar manipulator used in computer simulations.

where D_j is an $m \times m$ matrix. Substituting (24) into (15), we obtain

$$(J^+_{M-1})^T D_j D_j^T = 0. \tag{25}$$

Since D_j is not a zero matrix, the following equation must hold:

$$(J^+_{M-1})^T D_j = 0. \tag{26}$$

The desired joint inertia matrix M_j^* is naturally assumed to be given as a positive semidefinite matrix, so it is also expressed as $M_j^* = (D_j^*)(D_j^*)^T$. Using the weighting matrix W and replacing M_j with D_j, we can derive the optimal solution D_j of the matrix equation (26) in the same way as described in the previous subsection:

$$D_j = \Gamma D_j^*. \tag{27}$$

Then, substituting (27) into (24) and using $M_j^* = (D_j^*)(D_j^*)^T$, we can obtain the following optimal joint inertia matrix:

$$M_j = \Gamma M_j^* \Gamma^T \tag{28}$$

which is the closest to the desired inertia M_j^* in the class of positive semidefinite matrices satisfying (15).

Also the joint viscosity matrix B_j and the joint stiffness matrix K_j can be derived as

$$B_j = \Gamma B_j^* \Gamma^T, \tag{29}$$

$$K_j = \Gamma K_j^* \Gamma^T. \tag{30}$$

Consequently, the additional joint controller (14) with the inertia, viscosity and stiffness matrices given in (28)–(30) guarantees the stability of the joint motion of the manipulator.

IV. Computer Simulations and Experiments

A. Numerical Examples

The realized joint stiffness matrix K_j was computed using the proposed method for a four-joint planar manipulator of Fig. 3, where the link parameters of the manipulator are shown in Table I.

Table II shows the computed joint stiffness matrices and the index $E(K_j)$ which is defined in order to measure how close the realized joint stiffness K_j approaches the desired one K_j^*

$$E(K_j) = (\mathrm{tr}[(K_j^* - K_j)^T (K_j^* - K_j)])^{1/2}. \tag{31}$$

From Table II, it can be seen that the realized joint stiffness matrices reflect the corresponding desired ones. Also for

TABLE I
LINK PARAMETERS OF THE FOUR-JOINT PLANAR MANIPULATOR OF FIG. 2

	Link i (i = 1,2,3,4)
Length (m)	0.20
Mass (kg)	1.57
Center of mass (m)	0.10
Moment of inertia (kgm^2)	0.80

TABLE II
JOINT STIFFNESS MATRICES REALIZED BY THE PROPOSED METHOD

Types	Desired joint stiffness matrix, K_j (Nm/rad)	Weighting matrix, W	Realized joint stiffness matrix, K_j (Nm/rad)
(a) Hierarchical impedance control, Eq. (23)	100.0 0.0 0.0 0.0 0.0 10.0 0.0 0.0 0.0 0.0 10.0 0.0 0.0 0.0 0.0 100.0	1.0 0.0 0.0 0.0 0.0 1.0 0.0 0.0 0.0 0.0 1.0 0.0 0.0 0.0 0.0 1.0	58.0 0.3 2.7 41.1 3.2 2.7 -3.6 25.1 27.1 -3.6 6.6 -13.2 41.1 2.5 -1.3 48.7 $E(K_j)$ = 97.1 (Nm/rad)
	100.0 0.0 0.0 0.0 0.0 10.0 0.0 0.0 0.0 0.0 10.0 0.0 0.0 0.0 0.0 100.0	1.0 0.0 0.0 0.0 0.0 10.0 0.0 0.0 0.0 0.0 1.0 0.0 0.0 0.0 0.0 10.0	3.7 -11.7 0.4 142.5 -1.2 9.4 -0.2 3.4 3.6 -19.7 0.5 72.8 1.4 0.3 0.1 97.2 $E(K_j)$ = 188.6 (Nm/rad)
(b) Hierarchical impedance control with positive semi-definite joint impedance, Eq. (30)	100.0 0.0 0.0 0.0 0.0 10.0 0.0 0.0 0.0 0.0 10.0 0.0 0.0 0.0 0.0 100.0	1.0 0.0 0.0 0.0 0.0 1.0 0.0 0.0 0.0 0.0 1.0 0.0 0.0 0.0 0.0 1.0	51.3 11.3 11.9 43.6 11.3 8.4 -5.8 14.7 11.9 -5.8 14.8 2.9 43.6 14.8 2.9 41.5 $E(K_j)$ = 103.4 (Nm/rad)
	100.0 0.0 0.0 0.0 0.0 10.0 0.0 0.0 0.0 0.0 10.0 0.0 0.0 0.0 0.0 100.0	1.0 0.0 0.0 0.0 0.0 10.0 0.0 0.0 0.0 0.0 1.0 0.0 0.0 0.0 0.0 10.0	216.9 -6.2 127.1 138.3 -6.2 9.0 -16.2 3.6 127.1 -16.2 92.2 70.2 138.3 3.6 70.2 94.6 $E(K_j)$ = 318.6 (Nm/rad)

the large diagonal elements of the weighting matrix W, the elements in the corresponding row of K_j approach closer to the desired values than the ones in other rows. It should be noted that K_j in Table II(a) is not symmetric. On the other hand, as seen in Table II(b), K_j is always symmetric and positive semidefinite, although the discrepancy between K_j^* and K_j increases as indicated by the value of the index $E(K_j)$.

B. Computer Simulations

In the next step, computer simulations were performed using the four-joint planar manipulator shown in Fig. 3, where the desired end-point impedance matrices were M_e = diag.[1, 1] (kg), B_e = diag.[20, 10] (Ns/m), K_e = diag.[100, 400] (N/m). The damping ratios of the desired dynamic response for the end-point in the direction of x and y axes were 1.0 and 0.25, respectively, and the settling times of the end-point in the direction of x and y axes were 0.4 (s) and 0.8 (s), respectively. Also, in the proposed method, the desired joint impedance matrices were set as M_j^* = diag. [0.1, 0.1, 0.1, 0.1] (kgm^2), B_j^* = diag. [80, 8, 80, 8] (Nms/rad) and K_j^* = diag. [4000, 40, 4000, 40] (Nm/rad); and the weighting matrix was W = diag. [50, 1, 50, 1]. Moreover the desired end-point position X_d and the equilibrium joint angle θ_d were chosen as $X_d(t) = X(0)$ and $\theta_d(t) = \theta(0)$, respectively. The computations of the manipulator dynamics were performed using Appel's method [28].

Figs. 4 and 5 show the simulation results of the manipulator under the conventional impedance control method (3)–(5) and the proposed method (4)–(6), (14), (28)–(30), respectively, where the external torque disturbance, τ_{ext} = [40, 40, 40, 40]^T (Nm), is exerted to the joints of the manipulator.

In Fig. 4, all joints rotated and oscillated according to the torque disturbance, since no viscous friction was assumed for the rotation of all joints. It can be seen that the conventional

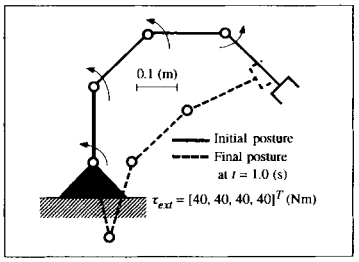

(a)

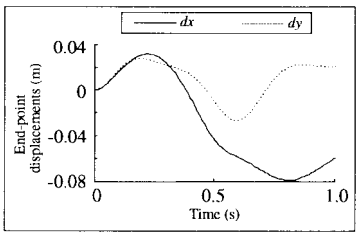

(b)

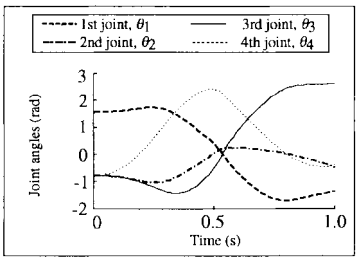

(c)

Fig. 4. Motion profile of the four-joint manipulator for the external torque exerted to the joints of the manipulator under the conventional impedance control: (a) stick pictures, (b) end-point displacements, and (c) joint angles.

end-point impedance controller used in this paper cannot resist the external joint torque disturbance. On the other hand, the first and third joints did not rotate in Fig. 5, since the desired impedance of the corresponding joints were set to be large. The proposed method is effective in resisting the unknown external joint torque disturbance.

Next, the proposed method was applied to a crank rotation task by a four-joint planar manipulator of Fig. 6. The link parameters of the manipulator are shown in Table III. Two kinds of coordinate systems were chosen:

1) world coordinate system $X(x, y)$;
2) polar coordinate system $\Phi(\phi, r)$ with its origin at the center of the crank, where ϕ is the rotational angle of the crank and r is the distance from the center of the crank to the end-point, i.e., the radius of the crank.

In Fig. 6, r = 0.15 m was used. Also, the viscous friction of each joint was set to 10.0 Nms/rad in order to avoid unstable results of the conventional impedance control.

The desired end-point impedance was expressed in the polar coordinate system, where the inertia, viscosity and stiffness matrices were chosen as M_e = diag. [2.25 $\times$ 10^{-3} (kgm^2), 0.1 (kg)]; B_e = diag. [0.45 (Nms/rad), 2 (Ns/m)]; and K_e = diag. [22.5 (Nm/rad), 10 (N/m)]. Also, the desired end-point

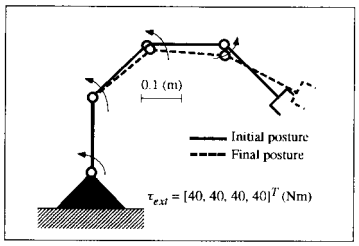

(a)

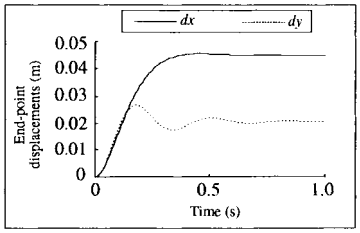

(b)

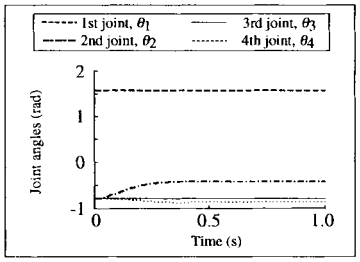

(c)

Fig. 5. Motion profile of the four-joint manipulator for the external torque exerted to the joints of the manipulator under the proposed method: (a) stick pictures, (b) end-point displacements, and (c) joint angles.

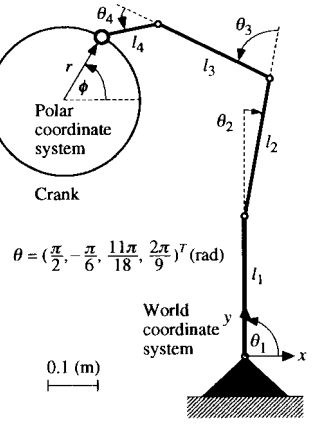

Fig. 6. The four-joint planar manipulator performing a crank rotation task.

trajectory, that is, the equilibrium trajectory, was defined as

$$\begin{bmatrix} \phi_d(t) \\ r_d(t) \end{bmatrix} = \begin{bmatrix} 20\pi t^3/t_f^3 - 30\pi t^4/t_f^4 + 12\pi t^5/t_f^5 \\ r \end{bmatrix} \quad (32)$$

where the time duration t_f was set to 2.0 s.

Figs. 7 and 8 show simulation results under the conventional impedance control method and the proposed method, respectively. The desired joint impedance matrices in (13) were set as $M_j^* =$ diag. [0.001, 0.0001, 0.0001, 0.001] (kgm^2); B_j^* = diag. [2, 0.2, 0.2, 2] (Nms/rad); and $K_j^* =$ diag. [1000, 100, 100, 1000] (Nm/rad) with the equilibrium joint trajectory $\theta_d(t) = \theta(0)$. The weighting matrix was set as $W =$ diag. [50, 1, 1, 50] in order to assign high priority to the impedance of the first and fourth joints.

TABLE III
LINK PARAMETERS OF THE FOUR-JOINT PLANAR MANIPULATOR OF FIG. 5

	Link 1, 2	Link 3	Link 4
Length (m)	0.28	0.25	0.11
Mass (kg)	3.392	1.92	1.152
Center of mass (m)	0.128	0.1025	0.055
Moment of inertia (kgm^2)	0.29312	0.011017	0.00123

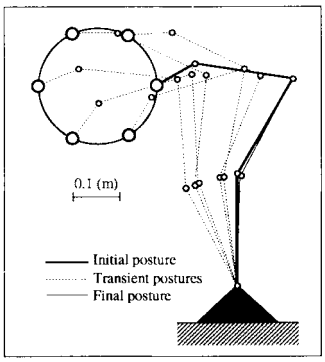

(a)

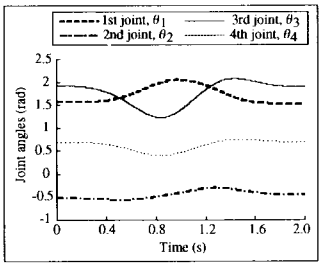

(b)

Fig. 7. Motion profile of the four-joint manipulator during the crank rotation task under the conventional impedance control: (a) stick pictures and (b) joint angles.

Although the manipulator can rotate the crank properly in both the cases, the effectiveness of the proposed method appears clearly in the joint motion. The first and fourth joints did not move during the crank rotation under the proposed method, since their impedances were set to be larger than the ones of other joints. As a result, the initial and final joint configurations were exactly the same, and the end-point motion was realized by using only the second and third joints.

C. Experiments

Finally, experiments using a three-joint direct-drive manipulator of Fig. 9 were performed, where the link parameters are shown in Table IV. The joint angles were measured by means of optical encoders (resolution: 1.745×10^{-5} rad) and the control law was implemented by using four CPU's (Transputer, T800, 25 MHz).

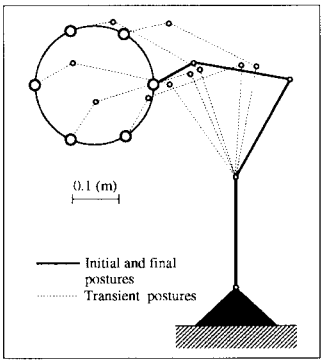

(a)

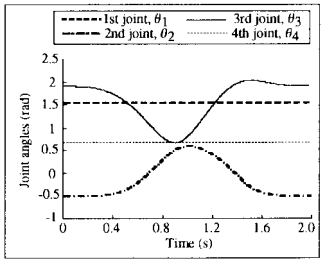

(b)

Fig. 8. Motion profile of the four-joint manipulator during the crank rotation task under the proposed method. The impedances of the first and fourth joints are set considerably larger than the ones of other joints: (a) stick pictures and (b) joint angles.

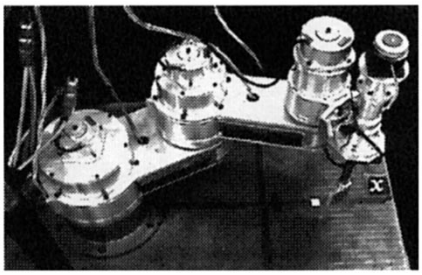

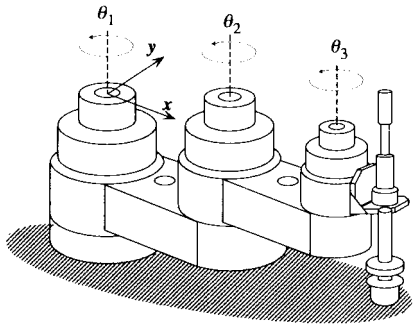

Fig. 9. Direct-drive robot used in the experiments.

Figs. 10–12 show the experimental results, where the desired end-point impedance matrices were $M_e = \text{diag.}[25, 25]$ (kg), $B_e = \text{diag.}[80, 80]$ (Ns/m), and $K_e = \text{diag.}[400, 400]$ (N/m). The damping ratio of the desired dynamic response of the end-point in each direction was 0.4. In Figs. 10 and 11, only the end-point impedance was controlled under the conventional impedance control (3)–(5), while the proposed method (4)–(6), (14), (28)–(30) was used in Fig. 12. For the proposed method, the desired joint impedance matrices were set as $M_j^* = \text{diag. } [0.1, 0, 0]$ (kgm^2), $B_j^* = \text{diag. } [20, 0, 0]$ (Nms/rad), and $K_j^* = \text{diag. } [1000, 0, 0]$ (Nm/rad). The unit matrix was used as the weight matrix W for simplicity. Also the desired end-point position $X_d(t)$ was 0.1 m in the direction of x axis from its initial position, while the equilibrium joint angle was fixed at the initial angle $\theta_d(t) = \theta(0)$. The sampling interval of the controller was 1.4 ms for both the conventional impedance control and the proposed method.

Both methods realized almost the same end-point trajectories as the one prespecified by the desired end-point

TABLE IV
LINK PARAMETERS OF THE DIRECT-DRIVE ROBOT

	Link 1	Link 2	Link 3
Length (m)	0.25	0.25	0.125
Mass (kg)	20.8	13.2	8.84
Center of mass (m)	0.064	0.065	0.031
Moment of inertia (kgm^2)	0.334	0.196	0.0851
Joint friction (Nms/rad)	2.69	1.88	0.0634

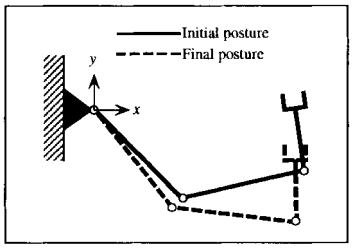

(a)

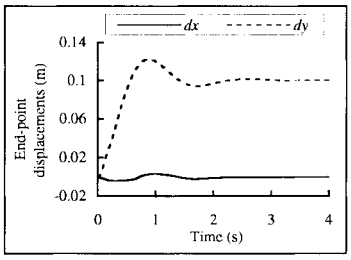

(b)

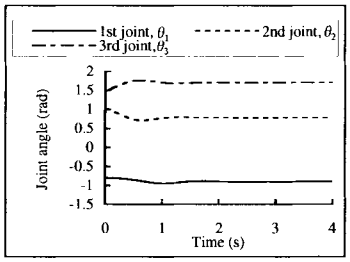

(c)

Fig. 10. Step response of the direct-drive robot under the conventional impedance control: (a) stick pictures, (b) end-point displacements, and (c) joint angles.

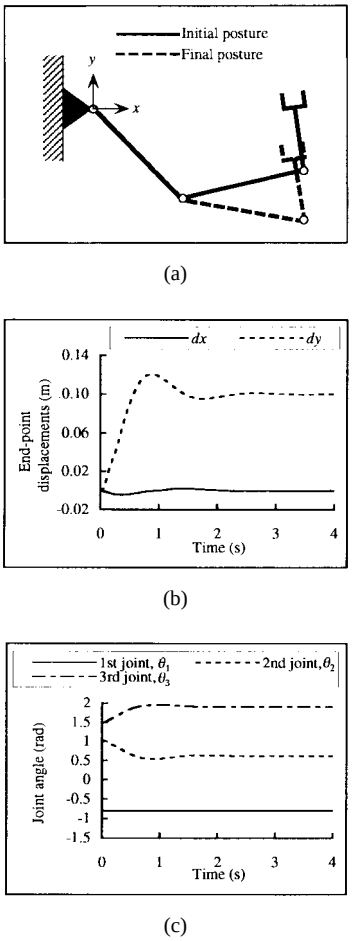

Fig. 11. Step response of the direct-drive robot under the proposed method, where the stiffness of the first joint is regulated considerably larger than the ones of other joints: (a) stick pictures, (b) end-point displacements, and (c) joint angles.

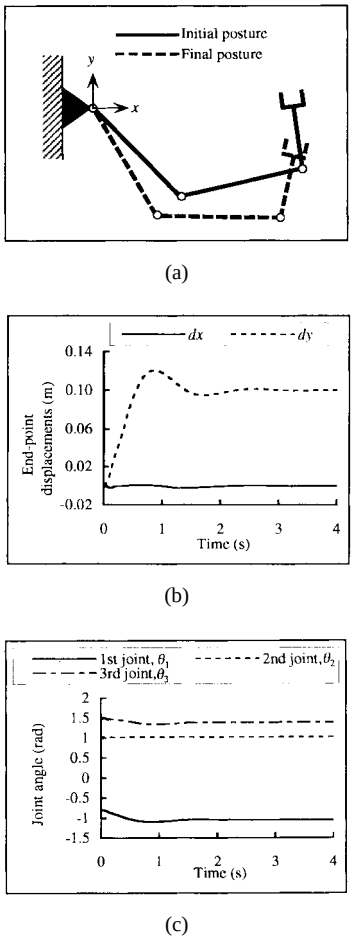

Fig. 12. Step response of the direct-drive robot under the proposed method, where the stiffness of the second joint is set considerably larger than the ones of other joints: (a) stick pictures, (b) end-point displacements, and (c) joint angles.

impedance. However, one of the joints was almost fixed in Figs. 11 and 12, which cannot be realized using any conventional impedance control method.

V. Conclusions

In this paper, we have proposed a new impedance control method that can effectively utilize arm redundancy in terms of the arm impedance by incorporating an additional controller to the end-point impedance controller. The distinctive feature of the proposed method is the ability to control not only the end-point impedance but also the joint impedance in such a way that it has no effects on the end-point motion of the manipulator. When the desired joint impedance is chosen adequately according to the task, the proposed method can realize the closest joint impedance in the least squares sense while still satisfying the desired end-point impedance.

Experimental verification of the proposed method has been done by using the direct-drive robot with sufficient accuracy. In order to reduce the control error, future research will be directed to develop a robust impedance control that can realize the desired arm impedance when the model of the manipulator is not precisely given.

Appendix

Let us consider the case of $W = I_m$ as the first step. In this case, the objective function (19) reduces to

$$G_1(Z_2) = ||M_j^* - M_j(Z_2)||. \tag{33}$$

Substituting (18) into (33), we find

$$G_2(Z_2) = (\mathrm{tr}[[M_j^* - \{I_m - \Omega(J_{M-1}^+)^T\}Z_2]^T \cdot [M_j^* - \{I_m - \Omega(J_{M-1}^+)^T\}Z_2]])^{0.5}. \tag{34}$$

The problem is how to find the matrix Z_2 that minimizes the objective function $G_2(Z_2)$. The necessary condition with regard to the optimal solution of the above problem is given by

$$\frac{\partial G_2(Z_2)}{\partial Z_2} = 0. \tag{35}$$

Substituting (34) into (35) and expanding it, we have

$$\{I_m - \Omega(J_{M-1}^+)^T\}Z_2 = \{I_m - \Omega(J_{M-1}^+)^T\}M_j^*. \tag{36}$$

Note that the partial differential formulas for the trace of matrices [29]

$$\frac{\partial \,\mathrm{tr}[PZ_2Q]}{\partial Z_2} = P^TQ^T, \tag{37}$$

$$\frac{\partial \,\mathrm{tr}[PZ_2^TQZ_2R]}{\partial Z_2} = QZ_2RP + Q^TZ_2P^TR^T \tag{38}$$

and the property of A^+, that is, $(A^+A)^T(A^+A) = (A^+A)^T = (A^+A)$, is used in the derivation of (36). Here, P, Q, and R are matrices with appropriate dimensions. Then, substituting (36) into (18), we obtain

$$M_j = \{I_m - \Omega(J_{M-1}^+)^T\}M_j^*. \tag{39}$$

The above equation gives the least squares solution of the matrix equation (15) with the objective function (33).

Next, we will derive the optimal solution for the general case, where the weighting matrix W is not the unit matrix. In this case, we rewrite the matrix equation (15) as follows:

$$(J_{M-1}^+)^TW^{-1}WM_j = (W^{-1}J_{M-1}^+)^TWM_j = 0. \tag{40}$$

Comparing (40) with (15), we can see that (40) has the same form as (15), in which $W^{-1}J_{M-1}^+$ and WM_j are corresponding to J_{M-1}^+ and M_j in (15), respectively. Therefore, the general solution of (40) for WM_j can be easily derived as

$$WM_j = [I_m - \{(W^{-1}J_{M-1}^+)^T\}^+(W^{-1}J_{M-1}^+)^T]Z_3 \tag{41}$$

where $\{(W^{-1}J_{M-1}^+)^T\}^+ = W^{-1}J_{M-1}^+\{(J_{M-1}^+)^TW^{-2}J_{M-1}^+\}^{-1} \in \Re^{m\times l}$ is the right-side generalized inverse of $(W^{-1}J_{M-1}^+)^T$ and $Z_3 \in \Re^{m\times m}$ is an arbitrary constant matrix.

Substituting (41) into (19) and finding the matrix Z_3 that minimizes the cost function, we have

$$\begin{aligned}&[I_m - \{(W^{-1}J_{M-1}^+)^T\}^+(W^{-1}J_{M-1}^+)^T]Z_3\\ &\quad = [I_m - \{(W^{-1}J_{M-1}^+)^T\}^+(W^{-1}J_{M-1}^+)^T]WM_j^*.\end{aligned} \tag{42}$$

Finally, substituting (42) into (41) and expanding it, we can get

$$\begin{aligned}M_j &= W^{-1}[I_m - \{(W^{-1}J_{M-1}^+)^T\}^+(W^{-1}J_{M-1}^+)^T]WM_j^*\\ &= \{I_m - \Omega_{W^{-2}}(J_{M-1}^+)^T\}M_j^*\\ &= \Gamma M_j^*,\end{aligned} \tag{43}$$

where $\Omega_{W^{-2}} = W^{-2}J_{M-1}^+\{J_{M-1}^+W^{-2}(J_{M-1}^+)^T\}^{-1} \in \Re^{m\times l}$ is the right-side generalized inverse of J_{M-1}^+ weighted by $W^{-2} \equiv W^{-1}W^{-1}$. Consequently, the objective function (19) is minimized by the optimal joint inertia matrix M_j of (21) as derived above.

REFERENCES

[1] N. Hogan, "Impedance control: An approach to manipulation, Parts I, II, III," *ASME J. Dyn. Syst. Contr.*, vol. 107, no. 1, pp. 1–24, 1985.

[2] ——, "Stable execution of contact tasks using impedance control," in *Proc. IEEE Int. Conf. Robot. Automat.*, 1987, pp. 1047–1054.

[3] S. Tachi, T. Sakaki, H. Arai, S. Nishizawa, and J. F. Pelaez-Polo, "Impedance control of a direct-drive manipulator without using force sensors," *Adv. Robot.*, vol. 5, no. 2, pp. 183–205, 1991.

[4] H. Kazerooni, T. B. Sheridan, and P. K. Houpt, "Robust compliance motion for manipulators, Parts i, ii," *IEEE J. Robot. Automat.*, vol. RA-2, pp. 83–105, June 1986.

[5] W. S. Lu and Q. H. Meng, "Impedance control with adaptation for robotic manipulation," *IEEE Trans. Robot. Automat.*, vol. 7, pp. 408–415, June 1991.

[6] E. Colgate and N. Hogan, "An analysis of contact instability in terms of passive physical equivalents," in *Proc. IEEE Int. Conf. Robot. Automat.*, 1989, pp. 404–409.

[7] Z. W. Luo and M. Ito, "Control design of robot for compliant manipulation on dynamic environments," *IEEE Trans. Robot. Automat.*, vol. 9, pp. 286–296, June 1993.

[8] A. Liegeois, "Automatic supervisory control of the configuration and behavior of multibody mechanism," *IEEE Trans. Syst., Man, Cybern.*, vol. SMC-7, pp. 868–871, Dec. 1977.

[9] C. A. Klein and C. Huang, "Review of pseudoinverse control for use with kinematically redundant manipulators," *IEEE Trans. Syst., Man, Cybern.*, vol. SMC-13, pp. 245–250, Mar./Apr. 1983.

[10] T. Yoshikawa, "Manipulability of robotic mechanism," *Int. J. Robot. Res.*, vol. 4, no. 2, pp. 3–9, 1985.

[11] A. A. Maciejewski and C. A. Klein, "Obstacle avoidance for kinematically redundant manipulators in dynamically varying environments," *Int. J. Robot. Res.*, vol. 4, no. 3, pp. 109–117, 1985.

[12] C. A. Klein, "Use of redundancy in the design of robotic system," in *Robotics Research: The Second International Symposium*, H. Hanafusa and H. Inoue, Eds. Cambridge, MA: MIT Press, 1985, pp. 207–214.

[13] J. Baillieul, "Avoiding obstacles and resolving kinematic redundancy," in *Proc. IEEE Int. Conf. Robot. Automat.*, 1986, pp. 1698–1704.

[14] O. Khatib, "A unified approach for motion and force control of robot manipulators: The operational space formulation," *IEEE J. Robot. Automat.*, vol. RA-3, pp. 43–53, Feb. 1987.

[15] ——, "Motion/force redundancy of manipulators," in *Proc. Japan–USA Symp. Flexible Automation*, 1990, vol. 1, pp. 337–342.

[16] H. J. Kang and R. A. Freeman, "Joint torque optimization of redundant manipulators via the null space damping method," in *Proc. IEEE Int. Conf. Robotics Automation*, 1992, pp. 520–525.

[17] W. S. Newman and M. E. Dohring, "Augmented impedance control: An approach to compliant control of kinematically redundant manipulators," in *Proc. IEEE Int. Conf. Robotics Automation*, 1991, pp. 30–35.

[18] Z. X. Peng and N. Adachi, "Compliant motion control of kinematically redundant manipulators," *IEEE Trans. Robot. Automat.*, vol. 9, pp. 831–837, Dec. 1993.

[19] Y. Oh, Y. K. Chung, Y. Youm, and I. H. Suh, "Motion/force decomposition of redundant manipulator and its application to hybrid impedance control," in *Proc. 1998 IEEE Int. Conf. Robotics Automation*, 1998, pp. 1441–146.

[20] T. Tsuji, K. Ito, and H. Nagaoka, "Identification and regulation of mechanical impedance for force control of robot manipulators," in *Proc. 11th Int. Federation Automatic Control World Congr.*, vol. 9, pp. 184–189, 1990.

[21] T. Tsuji, T. Takahashi, and K. Ito, "Multi-point compliance control for redundant manipulators," in *Advances in Robot Kinematics*, S. Stifter and J. Lenarčič, Eds. Berlin, Germany: Springer-Verlag, 1990, pp. 427–434.

[22] A. Jazidie, T. Tsuji, and K. Ito, "Multi-point compliance control of dual arm robotics," in *Proc. 1992 IEEE/RSJ Int. Conf. Intelligent Robots Systems*, 1992, pp. 65–70.

[23] T. Tsuji, A. Jazidie, and M. Kaneko, "Multi-point impedance control for redundant manipulators," *IEEE Trans. Syst., Man, Cybern. B*, vol. 26, pp. 707–718, Oct. 1996.

[24] C.-F. Liao and M. Donath, "Generalized impedance control of a redundant manipulator for handling tasks with position uncertainty while avoiding obstacles," in *Proc. 1997 IEEE Int. Conf. Robotics Automation*, 1997, pp. 1073–1079.

[25] J. K. Salisbury, "Active stiffness control of a manipulator or Cartesian coordinates," in *Proc. IEEE Conf. Decision Control*, 1980, pp. 95–100.

[26] R. J. Anderson and M. W. Spong, "Hybrid impedance control of robotic manipulators," *IEEE J. Robot. Automat.*, vol. 4, pp. 549–556, Oct. 1988.

[27] S. McMillan, D. E. Orin, and R. B. McGhee, "Efficient dynamic simulation of an underwater vehicle with a robotic manipulator," *IEEE Trans. Syst., Man, Cybern.*, vol. 25, pp. 1194–1206, Aug. 1995.

[28] V. Potkonjak and M. Vukobratovic, "Two new methods for computer forming of dynamic equation of active mechanisms," *Mech. Mach. Theory*, vol. 14, no. 3, pp. 189–200, 1987.

[29] M. Athans, "The matrix minimum principle," *Inf. Contr.*, vol. 11, pp. 592–606, 1967.

Toshio Tsuji was born in Kyoto, Japan, on December 25, 1959. He received the B.E. degree in industrial engineering in 1982, the M.E. and Dr.Eng. degrees in systems engineering in 1985 and 1989, all from Hiroshima University, Hiroshima, Japan.

From 1985 to 1994, he was a Research Associate in the Faculty of Engineering at Hiroshima University and was a Visiting Researcher of University of Genova, Genova, Italy, from 1992 to 1993. He is currently an Associate Professor in the Department of Industrial and Systems Engineering, Hiroshima University. He is interested in various aspects of motor control in robot and human movements. His current research interests have focused on the control of EMG-controlled prostheses, and computational neural sciences, in particular, biological motor control.

Dr. Tsuji is a member of Japan Society of Mechanical Engineers, Robotics Society of Japan, and Japanese Society of Instrumentation and Control Engineers.

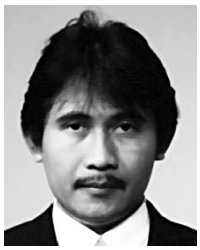

Achmad Jazidie received the B.S. degree in electrical engineering from Surabaya Institute of Technology, Surabaya, Indonesia, in 1984, the M.S. degree in information engineering and the Ph.D. degree in system engineering from Hiroshima University, Hiroshima, Japan, in 1992 and 1995, respectively. From 1989 to 1995, he was a recipient of graduate fellowships from the Hitachi Scholarship Foundation.

He is now a Lecturer in the Electrical Department, Faculty of Industrial Technology, Surabaya Institute of Technology. His main research interests are in kinematics, dynamics and control of multiple and redundant manipulator systems.

Makoto Kaneko (A'84–M'87) received the B.S. degree in mechanical engineering from Kyushu Institute of Technology, Kyushu, Japan, in 1976, and the M.S. and Ph.D degrees in mechanical engineering from Tokyo University, Tokyo, Japan, in 1978 and 1981, respectively.

From 1981 to 1990, he was a Researcher in the Mechanical Engineering Laboratory, Ministry of International Trade and Industry, Tsukuba Science City, Japan. From 1988 to 1989, he was a Postdoctoral Fellow at Technical University of Darmstadt, Darmstadt, Germany, where he joined the space robotics project. From 1990 to 1993, he was an Associate Professor of computer science and systems engineering at Kyushu Institute of Technology. From November 1991 to January 1992, he was an Invited Professor, Technical University of Darmstadt. Since October 1993, he has been a Professor, Industrial Engineering Department, Hiroshima University, Hiroshima, Japan. His research interests include tactile-based active sensing, grasping strategy, sensor applications, and experimental robotics.

Dr. Kaneko received the Outstanding Young Engineer Award in 1983 from the Japan Society of Mechanical Engineers, the Best Paper Award from the Robotics Society of Japan in 1994, and from the Japanese Society of Instrumentation and Control Engineers in 1996. He also received the Humboldt Research Award in 1997. He served as an Associate Editor of the IEEE TRANSACTIONS ON ROBOTICS AND AUTOMATION from 1990 to 1994. He has been a program committee member for IEEE International Conference on Intelligent Robots and Systems since 1991. He also worked as a program committee member for 1995, 1996, and 1998 IEEE International Conference on Robotics and Automation. He is a member of the IEEE Robotics and Automation Society, the IEEE Systems, Man, and Cybernetics Society, and the IEEE Industrial Electronics Society. He is also a member of Japan Society of Mechanical Engineers, Robotics Society of Japan, and Japanese Society of Instrumentation and Control Engineers.